

We are IntechOpen, the world's leading publisher of Open Access books Built by scientists, for scientists

4,800

Open access books available

122,000

International authors and editors

135M

Downloads

Our authors are among the

154

Countries delivered to

TOP 1%

most cited scientists

12.2%

Contributors from top 500 universities



WEB OF SCIENCE™

Selection of our books indexed in the Book Citation Index
in Web of Science™ Core Collection (BKCI)

Interested in publishing with us?
Contact book.department@intechopen.com

Numbers displayed above are based on latest data collected.

For more information visit www.intechopen.com



Application of Cubic Spline Interpolation Technique in Power Systems: A Review

Akhil Prasad, Atul Manmohan,
Prabhakar Karthikeyan Shanmugam and
Kothari D.P.

Additional information is available at the end of the chapter

<http://dx.doi.org/10.5772/intechopen.74853>

Abstract

In this chapter, a comprehensive review is made on the application of cubic spline interpolation techniques in the field of power systems. Domains like available transfer capability (ATC), electric arc furnace modeling, static var. compensation, voltage stability margin, and market power determination in deregulated electricity market are taken as samples to illustrate the significance of cubic spline interpolation.

Keywords: power systems, available transfer capability, electric arc furnace, thyristor-controlled reactor, voltage stability, market power

1. Introduction

With electricity becoming an inevitable part of all spheres of human life, it is imminent that the increasing demand for electricity be met. The realization of this necessity has manifested in extensive research in the field of power systems, which has brought to light the complexity of power system. The power system involves the continuous variation in connected loads and increases in power requirement which demands a corresponding increase in the generation. This is met via several means most recently characterized by the penetration of renewable energy sources. The unpredictability of these events entails the deployment of probabilistic-based load flow techniques, estimation of unknown variables and load models which includes uncertainties for their analysis.

All the analysis and research aimed at providing solutions or mitigating the above-mentioned problems require vast amounts of data which is discrete in nature or the analysis techniques involve responses that are discrete in nature. Regardless of the origin of this non-continuity of data, obtaining a continuous response is imperative because of the desired accuracy and the continuity of real-time operation.

The challenges set the stage for interpolation techniques to play an active role in mitigating the problems prevailing in the current power system studies like load forecasting, power system reactive power planning, transmission network expansion, available transfer capability (ATC) determination and market power/clearing price forecasting. Among the various interpolation techniques available, the cubic spline method has been found to be a popular method. Cubic spline also has the desirable characteristics of continuous derivatives at data points which make the design of controllers around these regions possible, and its employment has been seconded by the high accuracy obtained.

The measurements we take for analysis in everyday life are wrought with noise that may be caused by the surrounding environment. Especially in electrical measurements, such random noises may be caused by the magnetic field produced by the current, the presence of stray charges, heating caused by the flow of eddy currents, and so on. One of the possible solutions to the problems caused by noise is to take a large number of measurements. This ensures that the random noise gets canceled out on an average, and hence the integrity of the data is maintained. Other complicated methods of tackling the errors caused by noise are available, but the detailed and in-depth analysis of these methods falls beyond the scope of this chapter.

2. Determination of available transfer capability

The first application of cubic splines is in finding the available transfer capability, which is an important parameter in power system operation. Ever since the advent of the deregulated power system, the computation of transfer capability has been a priority. Two quantities that require special attention in these computations are the total transfer capability (TTC) and the available transfer capability (ATC). The TTC of a power system is defined as the maximum amount of power that can be transferred over the interconnected transmission network in a reliable manner while meeting all of a specific set of defined pre- and post-contingency system conditions [1]. ATC is defined as the measure of the additional amount of power that may flow over and above the base case flows without jeopardizing power system security [1]. The system operators of the deregulated power system normally can obtain previously calculated ATC values through an open-access same-time information system. However, the need for a quick calculation of ATC poses a challenge. Some of the methods employed include DC power flow, AC power flow, optimal power flow and sensitivity. Most of the methods mentioned earlier are not sufficiently agile as far as computation speed is concerned or trades accuracy for speed. For example, DC power flow yields quick results at the expense of accuracy, whereas AC power flow compromises speed for accuracy. A solution to the abovementioned problem is found by employing curve-fitting techniques especially the cubic spline interpolation technique.

In order to compute ATC, the cubic spline is employed to trace the curve of the variation of voltage magnitude and power flow with respect to the real power transfer. The ATC is then determined by the point where the limits of voltage magnitude or power flow intersect the curves. The computation of ATC takes place in two different forms—the point-to-point ATC and area-to-area ATC. The area-to-area ATC refers to the additional power that can be mobilized from the seller area to the buyer area, whereas the point-to-point ATC refers to bus-to-bus transfer (usually from a generating bus to a load bus). Another factor considered of paramount importance for the computation of ATC is the effect of contingencies like line outages. Individual consideration of line outages for a large-scale power system is an impractical approach, and hence contingency analysis is carried out using contingency ranking which helps select the critical lines.

The mathematical definition of ATC is shown in Eq. (1):

$$ATC = TTC - TRM - ETC - CBM \quad (1)$$

The definition of the abovementioned terms is as follows:

Transmission reliability margin (TRM): the amount of transmission capability necessary to ensure the security of the interconnected system under a reasonable range of uncertainties in the system.

Capacity benefit margin (CBM): the amount of transmission capability reserved by load-serving entities to ensure access to generation from interconnected systems to meet generation reliability requirements.

Existing transmission commitments (ETC): normal transmission flows.

Traditionally, ATC computation involves the recursive application of AC power flow with increasing power transfers, thereby tracing voltage magnitudes and MVA power flow variations with respect to real power formally called the P-V and the P-S curves as shown in **Figure 1**. These curves are then employed in conjunction with the limits imposed by acceptable voltage magnitudes and power flows to calculate the ATC. In the cubic spline-based approach, the cubic spline interpolation technique is used to trace the P-V and P-S curves which are then

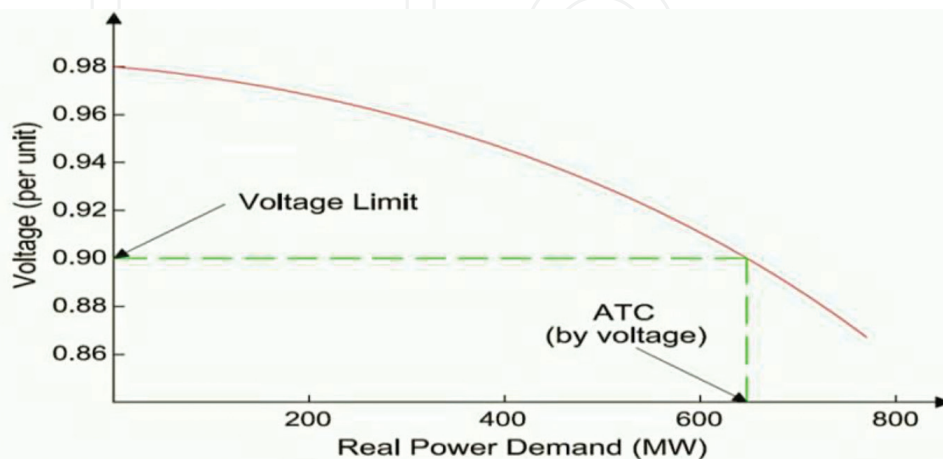


Figure 1. Variation of voltage with real power transfer.

employed to calculate the ATC. This is done by first determining four known points on the curve using AC power flow and then using cubic spline interpolation to trace the curves in between those points. The four known points are denoted as $V_i(P_n)$ and $S_{ij}(P_n)$, where V_i is for voltage of bus 'i', S_{ij} is the MVA power flow between bus 'i' and 'j', P_n is the real power transfer and n is the index for the four points and has values of $n = 1, 2, 3$ and 4 . The incremental steps for tracing the P-V or the P-S curve will be of 1 MW each.

The first and foremost step in the process of curve tracing consists of the determination of the four points on the P-V and P-S curves. This is of paramount importance because the power system undergoes voltage collapse once the real power transfer crosses a certain limit. In the voltage collapse process, the particular bus faces a continuous drop in bus voltage once the critical point load is exceeded. Therefore, the points must be selected carefully making sure that the critical point is not exceeded.

2.1. Procedure to calculate ATC

Step 1. Perform the line contingency ranking using line-loading performance index (PI_{MW}) and bus voltage performance (PI_v). This is done to identify the critical lines. The critical lines will have a PI value greater than $PI_{base\ case}$.

Step 2. Find a base case by solving the AC load flow. This will act as the first point.

Step 3. Perform the simulation for line outage for one of the critical lines found in step 1.

Step 4. Specify the point or area of transfers. For the point-to-point transfer, generally a generator bus is taken as the selling bus and a load bus as the buying bus. On the other hand, for area-to-area transfer, all the generator busses in a particular area called the selling area and all the load busses in a specific buying area are considered.

Step 5. Now, the next three points are determined. The first step is to determine the fourth and final point P_4 . In order to do so, the sensitivity method is employed. This method is based on the limiting point of system constraints which is given in Eqs. (2)–(4)

$$PT_{i,V_L} = \left| \frac{\partial \lambda}{\partial V_i} \times (V_L - V_i^0) \right| \quad (2)$$

$$PT_{i,V_U} = \left| \frac{\partial \lambda}{\partial V_i} \times (V_U - V_i^0) \right| \quad (3)$$

$$PT_{ij,S} = \left| \frac{\partial \lambda}{\partial S_{ij}} \times (S_{ij}^{limit} - S_{ij}^0) \right| \quad (4)$$

In Eqs. (2)–(4), PT_{i,V_L} , PT_{i,V_U} and $PT_{ij,S}$ are the estimates of P_4 which are arrived at by using the linear estimates based on the lower voltage limit, the upper voltage limit and the thermal limit of each line, respectively. The lower limit of voltage V_L is taken as 0.9 p.u. and the upper limit V_U is taken as 1.1 p.u. S_{ij}^{limit} is the thermal limit of each line. V_i^0 and S_{ij}^0 are the base case values computed in step (ii). The derivative terms are the reciprocal of the rate of change of voltage and MVA power flow with real power. This can be obtained by solving the AC power flow starting from the base case and making a small change in the transferred real power and

noting the change in voltage and MVA transfer. The fourth known point P_4 is selected as the minimum of all three values computed above. Then, based on this, P_2 and P_3 are chosen using the formulae given in Eqs. (5) and (6)

$$P_2 = \frac{P_4}{3} \quad (5)$$

$$P_3 = P_2 \times 2 \quad (6)$$

Step 6. Now, find the MVA and bus voltage V_i for each of the newly computed real power values— P_2 , P_3 and P_4 .

Step 7. Now, use the cubic spline to trace the curve in between these points and obtain the P-V and the P-S curves.

Now, the area-to-area and point-to-point ATCs are calculated by obtaining the point where the voltage limit or the MVA limit line intersects the P-V and P-S curves, respectively.

Inference: The author of [1] has employed the proposed cubic spline-based method to compute the ATC of the Malaysian power system. The performance of the method is measured in terms of its accuracy and speed (which are the main reasons for the employment of the method). For testing the Malaysian power system, it has been simplified into a 241-bus system and further classified into three regions namely north, east, central, south and PUB. The lower and upper voltage limits are taken as 0.9 and 1.1 p.u., respectively. The results obtained have been compared with the traditional recursive AC power flow results.

It is observed from the results obtained in [1] that all the ATC values obtained are due to the MVA limitation. It is further observed that the performance of the cubic spline interpolation method is comparable to the AC power flow method in terms of accuracy. The observation of paramount importance is that while the proposed method obtains the high accuracy as found in the recursive AC power flow method, the time it requires to compute the ATC is much smaller than the AC recursive power flow method—to the extent that in some cases, the time required is up to 30 times lesser. Therefore, it may be concluded that the cubic spline method is superior to AC power flow in terms of speed and superior to DC power flow in terms of accuracy.

3. Electric arc furnace modeling

In this section, cubic spline is applied in modeling a very complex load—electric arc furnace (EAF). This example presents the true power of cubic splines in tracking extremely complex trajectories. The electric arc furnace's (EAF) ability to efficiently smelt scrap iron raw materials has made it the backbone of the steel-making industries. The EAF employs high temperatures produced by low-voltage and high-current electric arcs to smelt scrap iron raw materials. The increase in productivity requirements has led to EAFs being designed for high-power applications. The operation of EAFs introduces a significant amount of harmonics, inter-harmonics and flickers in the supply system. Therefore, it is mandatory that the operators pay much attention to the power-quality considerations. In order to study these problems, it is of paramount

importance to understand the nonlinear load characteristics that the EAF present to the power system. Also, in order to mitigate the power-quality issues and to further study the impact of EAFs on the power system, it is required that the EAF be modeled after obtaining its time response.

The entire operation of the EAF involves three stages namely striking, smelting and refining. In the striking process, the electric arc is built up by lowering the electrodes of all three phases, the melting process involves the melting of the material and the process ends with the stable refining. Due to the complexities involved in modeling the EAF operation in the striking and the melting processes, most of the research has been directed towards a steady-state modeling of the EAF in the refining stage of operation. The modeling of an EAF requires several parameters such as arc voltage, arc length and arc current, which are determined by the position of electrodes. Therefore, in order to accurately model the EAF, we need to know the field measurements of the electric response which involves the variation of voltage and current. The measured responses are then employed to develop an EAF conductance model using the cubic spline interpolation method.

The EAF is modeled as a function of nonlinear conductance using the cubic spline interpolation technique which is called the cubic spline interpolation model (CSIM). In this method, a set of cubic polynomials are obtained which helps understand the voltage–current characteristic of the EAF.

The steps involved are as follows:

First, a set of ‘ n ’ measured data points of conductance is obtained for one fundamental cycle of operation. The measurements lying in the interval $[a, b]$ such that $a = x_0 < x_1 < \dots < x_n = b$. For the interval between two adjacent points, a cubic function is defined as shown in Eq. (7).

$$G_i(x) = a_i + b_i(x-x_i) + c_i(x-x_i)^2 + d_i(x-x_i)^3 \quad (7)$$

where $i = 0, 1, 2, \dots, n-1$. The coefficients a_i, b_i, c_i and d_i are unknown. These coefficients need to be determined based upon the following constraints:

Step 1. Each spline must pass through the given data points y_i .

$$G_i(x_i) = y_i \text{ and } G_{n-1}(x_n) = y_n$$

Step 2. Interior data points between each spline must be continuous.

$$G_{i+1}(x_{i+1}) = G_i(x_{i+1})$$

Step 3. The first and the second derivatives of the splines must be continuous across the interior data points. Therefore, the spline forms a smooth function.

$$G'_{i+1}(x_{i+1}) = G'_i(x_{i+1}).$$

$$G''_{i+1}(x_{i+1}) = G''_i(x_{i+1})$$

Step 4. In addition to the conditions mentioned in steps 1–3, another boundary condition must be satisfied which concerns the derivative of the functions at the boundaries (at $x_0 = a$ and $x_n = b$). There are two types of boundary conditions that may be required to satisfy:

Natural boundary condition: $G''_0(x_0) = G''_{n-1}(x_n) = 0$.

Clamped boundary condition: $G'_0(x_0) = D_0$ and $G'_{n-1}(x_n) = D_n$.

where D_0 and D_n are the values of the first derivatives of the unknown functions.

It is generally found that the natural boundary conditions give less accurate results than the clamped boundary conditions. Alternately, one could possibly apply a boundary condition called not-a-knot condition, which in addition to the natural boundary condition also incorporates another condition that the third derivative of the function must be continuous at x_1 and x_{n-1} .

In order to find the coefficients— a_i , b_i , c_i and d_i —we follow the following steps and equations:

Step 1. Set $a_i = y_i$ for $i = 0, 1, 2, \dots, n$.

Step 2. Solve

$$\begin{aligned} & (h_0 + 2h_1)c_1 + (h_1 - h_0)c_2 \\ &= \frac{3}{h_0 + h_1} \left[(a_2 - a_1) - \frac{h_1}{h_0} (a_1 - a_0) \right], \quad \text{for } i = 1 \end{aligned} \quad (8)$$

and

$$\begin{aligned} & h_{i-1}c_{i-1} + 2c_i(h_{i-1} + h_i) + h_ic_{i+1} \\ &= \frac{3}{h_i} (a_{i+1} - a_i) - \frac{3}{h_{i-1}} (a_i - a_{i-1}), \quad \text{for } i = 2, \dots, n - 2 \end{aligned} \quad (9)$$

and

$$\begin{aligned} & (h_{n-2} - h_{n-1})c_{n-2} + (2h_{n-2} + h_{n-1})c_{n-1} \\ &= \frac{3}{h_{n-1} + h_{n-2}} \left[\frac{h_{n-2}}{h_{n-1}} (a_n - a_{n-1}) - (a_{n-1} - a_{n-2}) \right], \end{aligned} \quad (10)$$

where, $h_i = x_{i+1} - x_i$, for $i = 1, 2, \dots, n-1$

where $h_i = x_{i+1} - x_i$, for $i = 1, 2, \dots, n-1$.

Step 3. Set

$$c_0 = c_1 + \frac{h_0}{h_1} (c_1 - c_2), \quad (11)$$

$$c_n = c_{n-1} + \frac{h_{n-1}}{h_{n-2}} (c_{n-1} - c_{n-2}), \quad (12)$$

Step 4. Set

$$b_i = \frac{1}{h_i} (a_{i+1} - a_i) - \frac{h_i}{3} (c_{i+1} + 2c_i), \quad \text{for } i = 0, 1, 2, \dots, n-1 \quad (13)$$

Step 5. Set

$$d_i = \frac{1}{3h_i} (c_{i+1} - c_i), \quad \text{for } i = 0, 1, 2, \dots, n-1 \quad (14)$$

The coefficients a_i can be found in step 1. The coefficients c_i can be calculated by solving the linear equations developed in Eqs. (8)–(10). Then, finally coefficients b_i and d_i may be obtained from steps 4 and 5 (Eqs. (13) and (14), respectively).

Inference: The author in [2] has analyzed the performance of CSIM on an actual power system model developed in MATLAB/SIMULINK whose online diagram is also presented in [2]. The results obtained via employing the CSIM (shown in **Figure 4**) are then compared with the results obtained via employing two traditional methods namely (i) harmonic current injection model (HCIM), shown in **Figure 2**, and (ii) harmonic voltage source model (HVSM), shown in **Figure 3**. The results described in [2] have been obtained for three different parts—early,

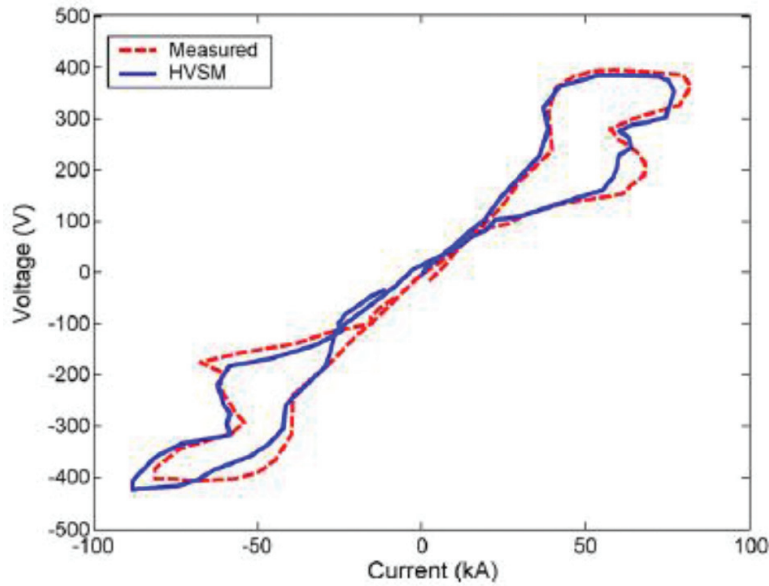


Figure 2. HVSM V-I characteristic [2].

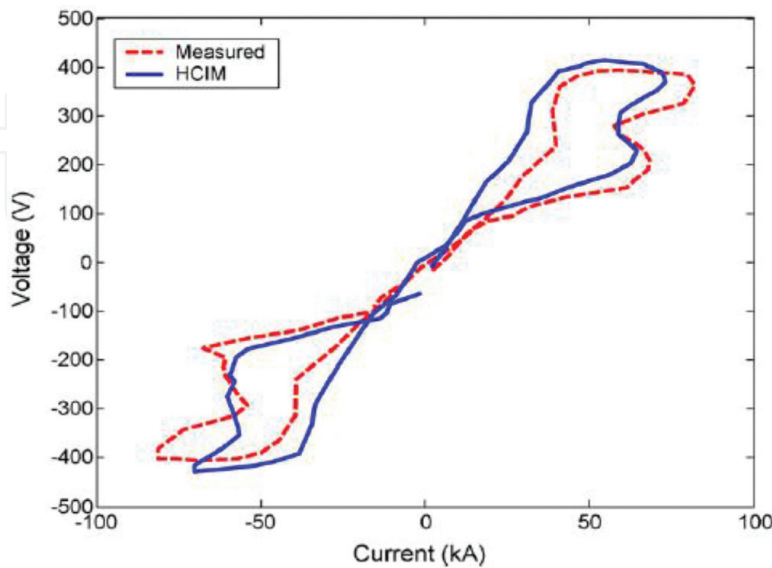


Figure 3. HCIM V-I characteristic [2].

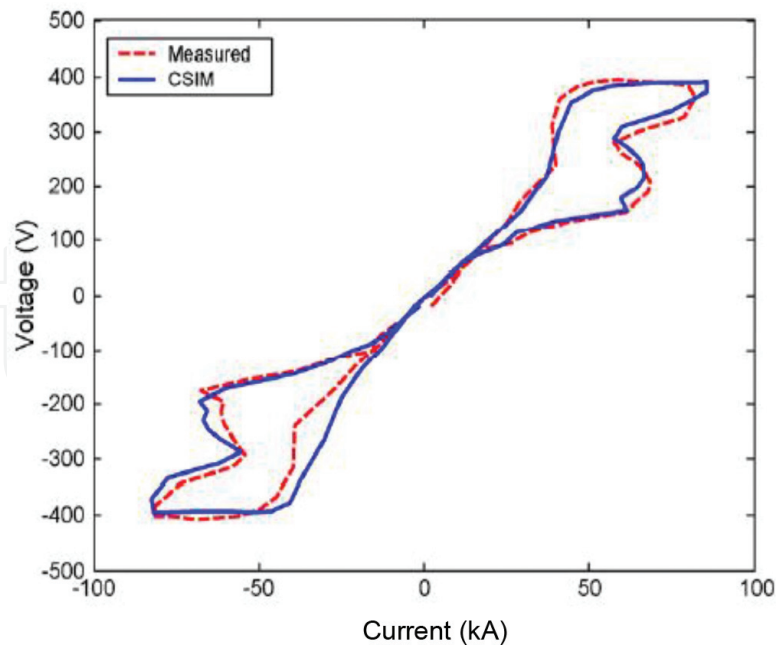


Figure 4. CSIM V-I characteristic (later stage) [2].

middle and later stages—of EAF operation during the refining period. This is done primarily because EAF does not possess a steady-state behaviour that lasts long. Since the HCIM and HVSM are unable to model dynamic behaviour, these methods are compared with the CSIM only during the latter part of the operation because of the dynamic behaviour of the EAF in the early and middle parts (**Figure 4**).

Upon employing the CSIM for EAF modeling in the early and middle stages, it is found that the performance of the EAF during these stages is highly nonlinear. The V-I curve presents a multi-valued function which makes it difficult to model the EAF. The results shown in [2] suggest that upon the comparison, the HCIM method yields the largest errors in terms of both the EAF voltage and current determined. Then, HVSM, which albeit an improvement on HCIM, still contains errors. The proposed CSIM method performs better than HCIM and HVSM and provides a better fit for the voltage and current characteristics. It is also explained in the results that the error encountered during modeling using CSIM in the early and middle stages is larger when compared to that encountered when modeling the later stages of the refining period because the number of sampling points used for the EAF model is not sufficient for modeling in the early and middle stages of refining. As an extension, it is also proposed in [2] that the cubic spline interpolation technique can also be used for modeling other nonlinear loads.

4. Var compensator with thyristor-controlled reactor

The problem of maintaining a good power factor (greater than 0.85) is a challenge faced by most of the industries. Some of these bulk consumers are penalized for operation under a low power factor. The application of cubic splines is presented to topic address this challenge and

provide a commendable solution. Rolling mills and electric arc furnaces constitute very large loads in the power system. When the problem of power factor is considered, these loads (particularly electric arc furnaces) may be termed as a necessary evil because of their extremely low power factor. The variation in the arc length during operation results in the introduction of severe and rapid fluctuations in the reactive power and the voltage, and when the short circuit occurs, the power factor drops to values as low as 0.1. The large impact current and reactive power generated result in significant waste of energy and may also cause the power system to lose its stability. This may cause decadence in the quality of load and endanger the users. The solution to the abovementioned problem is cited in a process called reactive power consumption. Currently, the reactive power compensation is achieved dynamically by the placement of a dynamic reactive power compensation device at access points of such interference loads. These devices are usually represented as a fixed capacitor and thyristor-controlled reactor (FCT). The FCT enables smooth control of the reactive power and also has the desirable feature of maintaining its voltage unchanged. In addition, the FCT can effectively suppress voltage fluctuation and solve the voltage distortion and flicker problem and improve the power quality. The continuous and smooth variation in the reactive power is obtained by the variation of the thyristor conduction angle. For the FCT to effectively carry out its task, it is imperative that it calculates the control angle quickly and accurately in a real-time environment. However, the existence of a nonlinear relation between the control angle and the reactor amplification factor makes the real-time calculation a cumbersome process.

The remainder of this section reviews the calculation and the corresponding control of the control angle via employing cubic spline interpolation technique. The calculation of the control angle, α , is based on the reactor amplification factor for each phase. Cubic spline interpolation is employed because it provides a low-order polynomial interpolation polynomial and also increases the smoothness of the interpolation function.

The basic thyristor-controlled reactor (TCR) consists of a pair of anti-parallel thyristors in series with an inductor as shown in **Figure 5**. The thyristor delay angle varies between 90° and 180° . As a result, the fundamental current is completely reactive. An increase in the delay angle leads to a decrease in the fundamental reactive current, which is equivalent to increasing the reactance or reducing the susceptance and hence results in a decrease in the reactive power. Hence, the TCR can be seen as being equivalent to a variable susceptance which can be controlled using the delay angle ' α '. This is because the AC voltage remains constant but the

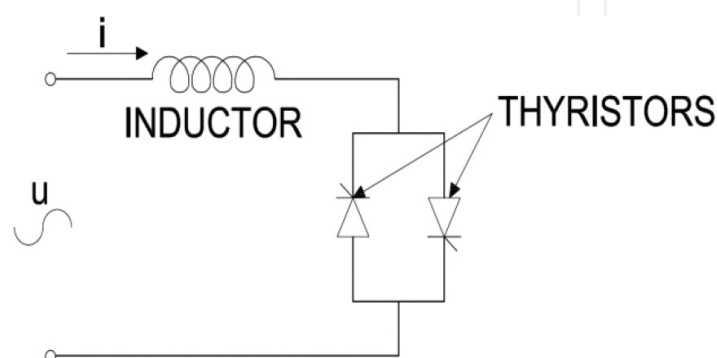


Figure 5. Thyristor controlled reactor.

value of the fundamental current changes, which in turn results in the variation in reactive power. The equivalent fundamental susceptance of the TCR is given in Eq. (15)

$$B_L(\alpha) = \frac{2\pi - 2\alpha + \sin 2\alpha}{\pi X_L} \quad (15)$$

The relationship between the delay angle, α , and the amplification factor of the equivalent impedance is shown in Eq. (16)

$$k = \frac{\pi}{2(\pi - \alpha) + \sin 2\alpha} \quad (16)$$

As can be seen, there exists a nonlinear relation between the delay angle and the amplification factor. The application of cubic splines makes the control of delay angle with reactive power variation easier, quicker and smoother. It must be observed that the inductance current in the TCR does not depend on the inductance but is rather governed by the thyristor conduction angle. The accurate control of the thyristor angle makes the accurate control of inductor current and hence reactive power possible.

The problem is formulated as follows. Eq. (9) suggests that in order to control the delay angle using the amplification factor 'k', we need to find a solution to the nonlinear equation. Albeit possible, it is a cumbersome task to solve nonlinear equations, not to mention the considerable amount of time the solving takes which make real-time application and control a tedious task. Moreover, of paramount importance is the accuracy of the controlling action since it determines the reactive power compensation. The cubic spline interpolation is employed as a means to calculate the control angle ' α ' having known the amplification factor 'k'. Cubic spline is used as the method of interpolation because of the advantages it provides in terms of simplicity of calculation, numerical stability and smoothness of the interpolated curve.

As previously stated, the existence of a nonlinear relation between the control angle and the amplification factor makes the real-time computation a lengthy process. In order to achieve the aim using cubic spline interpolation, the control angle is regarded as the dependent variable and the amplification factor 'k' as the independent variable. According to [3], the author generated 158 data points using Eq. (2). The aim is now to generate 157 interpolating cubic polynomials that fit in between these points. The form of these cubic polynomials is shown in Eq. (17)

$$\alpha = a_0(k - k_i)^3 + a_1(k - k_i)^2 + a_2(k - k_i) + a_3 \quad (17)$$

In Eq. (10), $i = 1, 2, \dots, 157$ and $k_i \leq k \leq k_{i+1}$.

The fitting coefficients a_0, a_1, a_2 and a_3 need to be computed for each interval which gives a unique cubic polynomial for each interval. When carrying out the control procedure first, the amplification is determined, and then the corresponding cubic polynomial is used to arrive at the required conduction angle value.

Inference: The results shown in [3] suggest that the conduction angle determined by using cubic splines shows significant match with the values obtained by simulation. Also, the use of cubic splines yields quicker results—a trait which would be beneficial for real-time applications.

Hence, it can be said that the cubic spline interpolation method is able to solve the problem of quick computation of the conduction angle with accuracies relevant to engineering applications.

5. Estimation of voltage stability margin

In this section, the application of cubic splines is of paramount importance since it marks the limit of a power system—the maximum amount of power that can be supplied before the continuous uncontrolled drop of voltage. The impact of voltage instability on the power system has been so damaging that significant research has been conducted in this direction. The phenomenon of voltage instability is characterized by a sudden and uncontrollable drop in voltage as a response to a disturbance that has occurred on the power system. This disturbance could be anything from the variation of load to loss of a line or lightning strike, and so on. Most of the studies have been focused on the steady-state aspect of voltage stability. In order to determine the proximity of the system to voltage collapse, we need to estimate or find the voltage stability margin (VSM). Many methods have been proposed in the past to estimate the steady-state voltage stability margin. One of the popular methods is the continuous power flow method. A major disadvantage of the continuous power flow is that it requires a considerable amount of time and hence it cannot be employed in real-time applications.

An alternative approach is to use the time-synchronized voltage and current phasor measurements obtained from phasor measurement units (PMUs). In the presented method, the author proposed a combination of a coupled single-port Thevenin equivalent model and cubic spline extrapolation in order to find the point of voltage collapse or the voltage stability margin (VSM). The concept is based on the fact that the voltage collapse point of the load impedance equals the Thevenin equivalent impedance.

Thevenin's equivalent voltage and equivalent impedance as seen from load bus 'i' as given in **Figure 6** can be written as shown in Eq. (18)

$$E_{\text{thi}} = [KV_G]_i - \sum_{j=1, j \neq i}^n Z_{ij} I_{Lj} \quad (18)$$

$$Z_{\text{thi}} = Z_{ii}$$

The definitions for the abovementioned variables can be found in [4].

The load impedance Z_{Li} of bus 'i' can be arrived by using Eq. (19)

$$Z_{Li} = \frac{V_{Li}}{I_{Li}} \quad (19)$$

The load bus voltage V_{Li} and the load bus current I_{Li} are obtained through the PMU measurements.

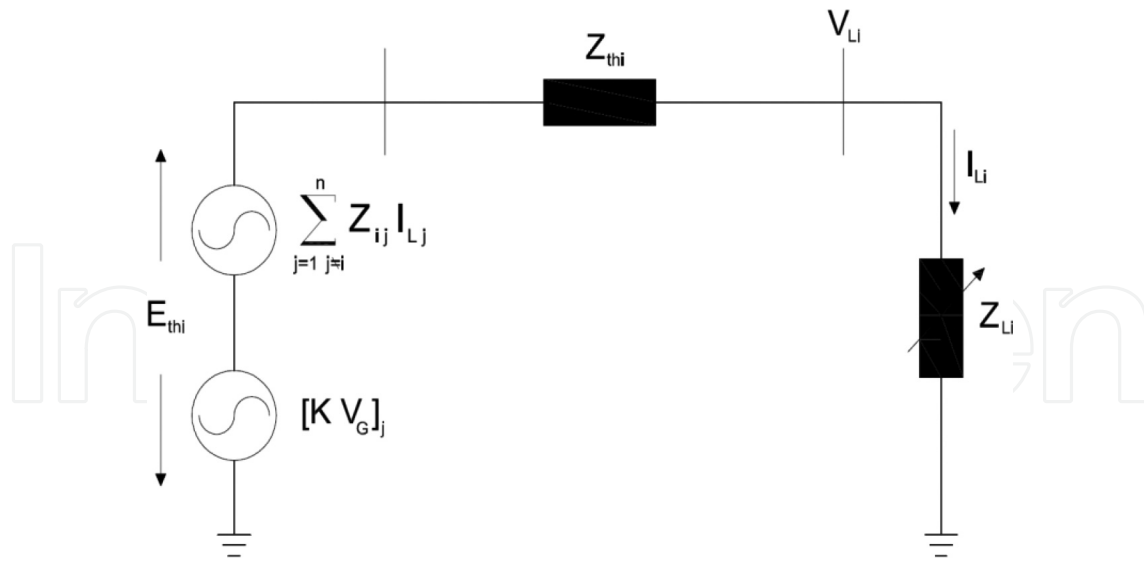


Figure 6. Coupled single port Thevenins' equivalent.

Figure 7 shows the variation of Z_{Li} and Z_{th} as a function of the load parameter λ . As can be seen, the Z_{Li} equals the Z_{th} at the point of maximum critical loading, and this point gives the maximum value of the load parameter— λ_{max} . This maximum value of load parameter can be arrived at by equating an approximate function that extrapolates the Z_{Li} versus λ curve to the point that it meets the Z_{th} line.

The choice of cubic spline extrapolation is justified by the author as the superior fitting to the impedance trajectory as evidenced by extensive simulation results. The cubic spline extrapolation proceeds by developing different cubic polynomials for the interval between measurements based on certain constraints.

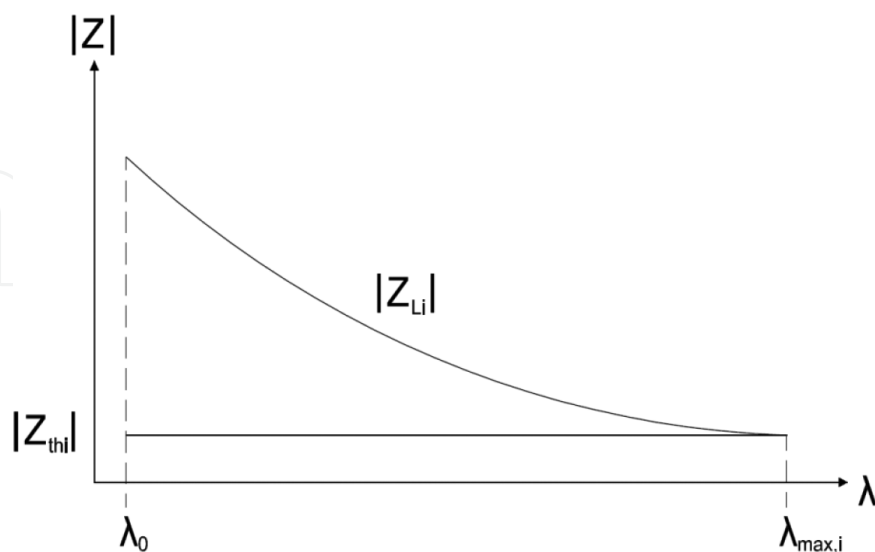


Figure 7. Variation of Thevenin and load impedance with λ [4].

For 'm' PMU-measured data points obtained, there will be 'm-1' intervals present, each of which is represented by Eq. (20)

$$f_j(x) = a_j + b_j(x - x_j) + c_j(x - x_j)^2 + d_j(x - x_j)^3 \quad (20)$$

The inputs for extrapolation are taken as three sets of $|Z_{Li}|$ and λ and the point of $|Z_{Li}|$ where λ is to be extrapolated and found. The λ thus found corresponds to the point where Z_{Li} equals Z_{thi} and hence is equal to λ_{maxi} . Each bus in the considered system will have its own corresponding λ_{max} s. The $\lambda_{max} = \lambda_{sys}$ for the entire system is found by taking the minimum of all λ_{maxi} obtained for each of the individual load busses. This value of λ_{sys} corresponds to the value of λ_{maxi} for the weakest load bus in the system. The proximity of the load bus to the voltage collapse point is given in Eq. (21)

$$VSM = \frac{\lambda_{sys} - \lambda_0}{\lambda_0} \times 100 \quad (21)$$

After the computation of VSM, the author of [4] proceeds to find an index which helps in determining whether the load increase results in the violation of the reactive power limits at the generator busses. The author begins with the simple power equation and arrives at the equation of a surface given by Eq. (22)

$$Q_G^2 - \frac{|V_G|^2}{X} Q_G + \frac{|V_G|^2}{X} Q_L + P_L^2 = 0 \quad (22)$$

where P_L , load real power; Q_L , load reactive power; Q_G , generator reactive power.

The surface defined lies in the (P_L, Q_L, Q_G) space. Upon cutting the surface with the constant power factor planes, we get the P_L - Q_G curves which are similar to PV curves or λV curves. The existence of an approximate quadratic relation between λ and V is extended to find a quadratic relation between λ and Q_G . This approximate quadratic relation is modeled and given in Eq. (23)

$$\lambda = \alpha_i Q_{Gi}^2 + \beta_i Q_{Gi} + \gamma_i \quad (23)$$

In Eq. (16), α_i , β_i and γ_i are parameters that are different for each generator bus and need to be determined. The parameters can be determined using three sets of PMU readings. Then, using the computed values of the parameters, an estimate for the extreme of Q_{Gi} is arrived using the condition that at the extreme limit $d\lambda/dQ_{Gi} = 0$ holds. Enforcing this condition gives us the following value as the estimate shown in Eq. (24)

$$Q_{Gi}^{ex} = -\frac{\beta_i}{2\alpha_i} \quad (24)$$

The index i stands for all the generator busses of the system. At each load step, it is ensured that the estimated value of generator reactive power— Q_{Gi}^{ex} —remains within the bounds of the reactive power limits that are specified for a generator bus.

The algorithm for proceeding with the described method in order to compute the VSM is as follows:

Step 1. Obtain three sets of PMU measurements and use them to compute three sets of $|Z_{Li}|$, λ and Q_{Gi} . Also, we possess the knowledge of the admittance matrix.

Step 2. Compute the parameters α_i , β_i and γ_i for each of the generator bus of the system.

Step 3. Compute the estimate of the extreme of the reactive power for each generator Q_{Gi}^{ex}

Step 4. If there is no violation of the reactive power limits of any generator, then proceed to step 6. Otherwise, proceed to step 5.

Step 5. Change the bus type from PV to PQ bus for the bus whose reactive power limit has been violated.

Step 6. Compute the impedance matrix as shown in [4].

Step 7. Compute the Thevenin equivalent impedance.

Step 8. Estimate the value of λ_{maxi} by using the cubic spline extrapolation technique for each load bus of the system.

Step 9. Find the value of λ_{sys} which is the minimum of all values computed in step 8.

Step 10. Determine the VSM.

Inference: The author of [4] has performed test runs of the proposed algorithm on the following test system—IEEE 30 bus system, IEEE 118 bus system and IEEE 300 bus system. Further, the obtained results have been compared with two other previously available methods. The obtained results indicate the superior performance of the proposed cubic spline technique when compared to the other methods. Upon comparison of the percentage error, it may be observed from [4] that the cubic spline method is almost 10 times more accurate than the other methods.

6. Estimation of market power in deregulated electricity market

In this final section, the application of cubic spline technique has been illustrated in the field of deregulated electricity market. In this market, market power issues predominantly spoil the basic idea of maintaining equilibrium within the market players.

Market power is the ability of showing one's monopolistic nature on the price of the commodities in the market. This has become a challenging issue in the context of the present electricity market and will become more challenging and play a significant role when private generation companies start participating in buying/selling the power [5]. Due to the increase in demand and the regulatory policies, private parties have started investing in the power sector, especially in the renewable energy sources. Thus, it is inevitable for the independent system operator (ISO) to estimate market power for taking crucial decisions [6].

